https://doi.org/10.5194/egusphere-2022-862
Preprint. Discussion started: 15 September 2022

Declining, seasonal-varying emissions of sulfur hexafluoride from the United States point to a new mitigation opportunity

Lei Hu[1,2*], Deborah Ottinger[3], Stephanie Bogle[3], Stephen Montzka[2], Phil DeCola[4,5], Ed Dlugokencky[2], Arlyn Andrews[2], Kirk Thoning[2], Colm Sweeney[2], Geoff Dutton[1,2], Lauren Aepli[5], Andrew Crotwell[1,2]

[1] Cooperative Institute for Research in Environmental Sciences, University of Colorado-Boulder, Boulder, CO, USA
[2] Global Monitoring Laboratory, US National Oceanic and Atmospheric Administration, Boulder, CO, USA
[3] Climate Change Division, US Environmental Protection Agency, Washington D.C., USA
[4] University of Maryland, College Park, MD, USA
[5] Gist.Earth LLC, College Park, MD, USA

*Correspondence to lei.hu@noaa.gov

Abstract

Sulfur hexafluoride (SF_6) is the most potent greenhouse gas and its atmospheric abundance, albeit small, has been increasing rapidly. Although SF_6 is used to assess atmospheric transport modeling and influences the climate for millennia, SF_6 emission magnitudes and distributions have substantial uncertainties. In this study, we used NOAA's ground-based and airborne measurements of SF_6 to estimate SF_6 emissions from the U.S. between 2007 and 2018. The substantial decline in U.S. SF_6 emissions derived from atmospheric observations agrees with the reported trend in the U.S. Environmental Protection Agency (EPA)'s national inventory submitted under the United Nations Framework on Climate Change, suggesting mitigation efforts have had some success. However, the magnitudes of derived annual emissions are 40 – 250% higher than the EPA national inventory and substantially lower than the Emissions Database for Global Atmospheric Research inventory. The regional discrepancies between atmosphere-based estimate and EPA's inventory suggest that emissions from electric power transmission and distribution (ETD) facilities and an SF_6 production plant that did not or do not report to EPA may be underestimated in the national inventory. Furthermore, the atmosphere-based estimates show higher winter than summer emissions of SF_6. These enhanced wintertime emissions may result from increased maintenance of ETD equipment in southern states and increased leakage through aging brittle seals in ETD in northern states in winter. These results demonstrate the success of past U.S. SF_6 emission mitigations, and suggest substantial additional emission reductions might be achieved through efforts to minimize emissions during servicing or through improving sealing materials in ETD.

Short Summary

Effective mitigation of greenhouse gas (GHG) emissions relies on an accurate understanding of emissions. Here we integrate inventory- and atmosphere- based approaches for estimating US emissions of SF_6, the most potent GHG known over a 100-year time-horizon. The results

https://doi.org/10.5194/egusphere-2022-862
Preprint. Discussion started: 15 September 2022

suggest a large decline in US SF_6 emissions, shed light on the possible processes causing the differences between the independent estimates, and identify opportunities for substantial additional emission reductions.

Introduction

Sulfur hexafluoride (SF_6) is a greenhouse gas (GHG) with the largest known 100-year global warming potential (GWP) (i.e., 25,200) and an atmospheric lifetime of 580 - 3200 years (Forster et al., 2021; Ray et al., 2017). SF_6 is primarily used in electrical circuit breakers and high-voltage gas-insulated switchgear in electric power transmission and distribution (ETD) equipment, and its emissions occur during manufacturing, use, servicing, and disposal of the equipment. There is also usage and associated emissions of SF_6 from production of magnesium and electronics. Because of its extremely large GWP and long atmospheric lifetime, emissions of SF_6 accumulate in the atmosphere and will influence Earth's climate for thousands of years. Since 1978, global emissions of SF_6 have increased by a factor of 4 due to rapid expansion of the ETD systems and the metal and electronics industries (Rigby et al., 2010; Simmonds et al., 2020). As a result, the global atmospheric mole fractions and radiative forcing of SF_6 have increased by 14 times over the same period. In 2019, the radiative forcing of SF_6 was 6 mW m^{-2} or 0.2% of total radiative forcing from all long-lived GHGs, making it the 11th largest contributor to the total radiative forcing among all the long-lived greenhouse gases and the 7th largest contributor among gases whose atmospheric concentrations are still growing (i.e., other than CFCs and carbon tetrachloride) (Gulev et al., 2021). If global SF_6 emissions continue at the same rate as 2018 (9 Gg yr^{-1}), the global atmospheric mole fraction and radiative forcing of SF_6 will linearly increase by another factor of 4 by the end of the 21st century (Fig. S1). If global emissions of SF_6 continue to rise at the same rate as 2000 – 2018, the global atmospheric mole fraction and radiative forcing of SF_6 will increase by another factor of 10 by the end of the 21st century (Fig. S1). Consistent with the large GWP of SF_6 emissions and its importance for influencing climate for many years after emissions, national emissions of this gas are reported under the United Nations Framework Convention on Climate Change (UNFCCC) annually. Furthermore, accurate estimates of emissions and distributions of SF_6 are also important in studies to refine our understanding of atmospheric transport processes in the troposphere and stratosphere (Orbe et al., 2021; Waugh et al., 2013; Denning et al., 1999; Gloor et al., 2007; Peters et al., 2004; Schuh et al., 2019; Ray et al., 2017).

Although global emissions of SF_6 can be well constrained with knowledge of its observed remote-atmosphere growth rates and its atmospheric lifetime, large uncertainties remain in the magnitude and distribution of SF_6 emissions on national and regional scales. For example, the total annual national emissions reported to the UNFCCC summed from developed countries and some developing countries (including one of the large SF_6 emitting countries such as China) account for only 50% of global annual SF_6 emissions derived from atmospheric observations for the analyzed years (1990 – 2007) (Simmonds et al., 2020; Rigby et al., 2010; Levin et al., 2010). This difference between activity-based inventory ("bottom-up") estimates and atmosphere-based ("top-down") estimates may result from underestimates of emissions by activity-based inventories (Simmonds et al., 2020; Rigby et al., 2010; Levin et al., 2010; Weiss and Prinn, 2011) as well as from substantial emissions from non-reporting countries. The results of activity-based inventories are sensitive to estimated activity levels and, especially, emission rates. In the Emission Database for Global Atmospheric Research version 6.0 (EDGARv6.0) (Janssens-Maenhout, 2011; Crippa et al.,

https://doi.org/10.5194/egusphere-2022-862
Preprint. Discussion started: 15 September 2022

2021), U.S. SF_6 emissions were up to five times larger than the emissions estimated by the U.S. Environmental Protection Agency (EPA) and in their reporting to the UNFCCC (Us Epa (United States Environmental Protection Agency), 2022b) (Fig. 1). This large difference likely stems from different input emission activity data and estimated emission factors used in these two inventory analyses. Uncertainties in EPA's emissions estimates were also illuminated by a comparison between the SF_6 usage inferred from the user reports (which form the basis of EPA's emissions estimates) and the SF_6 usage inferred from suppliers' reports, which showed that supplier-based estimates were 70% higher than user-based estimates in 2012 (Ottinger et al., 2015).

Against this backdrop, we estimated U.S. SF_6 emissions between 2007 and 2018 using atmospheric mole fraction measurements made from ground-based and airborne whole-air flask samples collected from the U.S. National Oceanic and Atmospheric Administration (NOAA) Global Greenhouse Gas Reference Network (Fig. 1) and a regional inverse model (Hu et al., 2019; Hu et al., 2021; Hu et al., 2017; Hu et al., 2016; Hu et al., 2015) (see Methods). The analysis provides robust emission estimates by region and season for the contiguous U.S. Our study offers an independent estimate that complements the current U.S. inventory-based national emission reporting of SF_6 to the UNFCCC. This effort exemplifies the quality assurance guidance laid out in the *2019 Refinement to the 2006 IPCC Guidelines for National Greenhouse Gas Inventories*, which states "Atmospheric measurements are being used to provide useful quality assurance of the national greenhouse gas emission estimates. Under the right measurement and modelling conditions, they can provide a perspective on the trends and magnitude of greenhouse gas (GHG) emission estimates that is largely independent of inventories" (Maksyutov et al., 2019). In fact, the United Kingdom, Switzerland, and Australia have already included top-down atmosphere-based emission estimates in the QA/QC section of their national GHG emission reporting to UNFCCC (Manning et al., 2017; Fraser et al., 2014; Henne et al., 2016). Derived national and regional SF_6 emissions from this analysis are accessible through NOAA's US Emission Tracker for Potent GHGs website (https://gml.noaa.gov/hats/US_emissiontracker) [note to editor and reviewers: this data will be posted at this link after acceptance].

Methods

Top-down atmosphere-based SF_6 emission estimates were derived using inverse modeling of NOAA's long-term atmospheric measurements of SF_6. Measurements made over North America were based on air samples collected by discrete flasks from tall towers and aircraft. The tall tower flask samples were typically collected every one to two days and airborne flask-sample profiles were collected once or twice per month between 0 and 8 km. Measurements made outside North America were from weekly whole-air samples collected globally, generally at remote locations far away from emission sources (https://gml.noaa.gov/dv/site/). All the whole-air flask samples were shipped to Boulder and analyzed by a Gas Chromatography with Electron Capture Detector (GC-ECD) for SF_6. Uncertainty of each SF_6 flask measurement is approximately 0.04 to 0.05 ppt, which includes uncertainties related to short-term measurement noise, long-term measurement reproducibility, and calibration scale transfer from gravimetric standards to working standards.

Mole fraction enhancements of SF_6 over the contiguous US (CONUS) (Fig. 1) relative to SF_6 mole fractions in air measured upwind were then estimated for deriving US emissions. These enhancements were estimated by referencing them to a "background" that was derived using three

https://doi.org/10.5194/egusphere-2022-862
Preprint. Discussion started: 15 September 2022

different approaches. These approaches are similar to previous inversion analyses for other atmospheric trace gases (Hu et al., 2021; Hu et al., 2017). In all three approaches, we constructed an empirical 4-dimensional mole fraction field based on measurements made in air over the Pacific and Atlantic Ocean basins and in free troposphere above 3 km over North America (Hu et al., 2017; Nevison et al., 2018), so that it contains vertical and horizontal gradients of mole fractions measured in the remote atmosphere over time. From this empirical background, we then extracted the mole fraction at the sampling time and location of each observation and used it as our first background estimate. In the second approach, we considered 500 air back-trajectories associated with each observation. Five hundred background estimates were extracted from this empirical background at locations when the air back-trajectories exited North America horizontally or vertically above 5 km. The 500 background estimates were averaged to obtain the background mole fraction estimation for that observation. In the third approach, we assessed potential biases in the background estimate from the second approach. Because there was a small fraction of back-trajectories ending up in the planetary boundary layer in North America back for 10 days and using the marine boundary layer information in the empirical background to estimate their mole fractions would likely result in an underestimate. To minimize such biases, we corrected our background estimates from the second approach based on their differences with measurements made within North America that had small surface sensitivities over populated areas, i.e. summed footprints over populated areas (areas with more than 10 persons km^{-2} less than 0.1 ppt (pmol m^{-2} s^{-1})$^{-1}$ (Hu et al., 2017).

SF_6 mole fraction enhancements estimated in observations at North American sites were then incorporated into a regional inverse model (Hu et al., 2019; Hu et al., 2021; Hu et al., 2017; Hu et al., 2016; Hu et al., 2015) to estimate US national and regional emissions. In regional inversions, we assume a linear relationship between atmospheric mole fraction enhancements and upwind emissions. The linear operator is called 'footprint' or the Jacobian matrix, representing the sensitivity of atmospheric mole fraction observations to emissions. It was computed by two transport models, the coupled Weather Research and Forecasting - Stochastic Time-Inverted Lagrangian Transport model (WRF-STILT) (Nehrkorn et al., 2010) and the Hybrid Single-Particle Lagrangian Integrated Trajectory model (Stein et al., 2015) driven by the North American Mesoscale Forecast System (HYSPLIT - NAMs). The WRF field has 41 pressure levels and a horizontal resolution of 10-km in North America and 40-km outside of North America. The NAMs meteorology has a 12-km resolution and 40 sigma-pressure levels. It was nested with the US National Centers for Environmental Prediction (NCEP) 0.5° Global Data Assimilation System (GDAS0.5) with 55 sigma-pressure levels. Both WRF-STILT and HYSPLIT-NAMs were run with 500 particles back in time for 10 days. Before March 2009, when NAMs was not available; we used NAM-12 meteorology, which has fewer vertical levels than NAMs. A Bayesian inverse modeling technique (Rodgers) was implemented, where a prior emission field or "a priori" was required. The model adjusts magnitudes and distributions of the a priori, such that the posterior solution of emissions better represents the observed magnitudes and horizontal and vertical gradients of mole fraction enhancements observed in the US. Here, we used two different temporally-constant prior emission fields, one from the Emissions Database for Global Atmospheric Research version 4.2 with a US total SF_6 emission of 1.8 Gg yr^{-1} (EDGARv4.2) and a second that includes a US total emission of 0.4 Gg yr^{-1} that has been distributed by population density from the Gridded Population of the World (GPW) v4 dataset (https://sedac.ciesin.columbia.edu/data/collection/gpw-v4, last access: 15 March 2019). The

https://doi.org/10.5194/egusphere-2022-862
Preprint. Discussion started: 15 September 2022

weight between the prescribed prior emissions and atmospheric observations in the final posterior emission solution was determined by the values in the prior emission error covariance matrix and the model-observation mismatch covariance matrix, which were calculated from the maximum likelihood estimation (Michalak et al., 2005; Hu et al., 2015).

A total of 12 inversion ensembles with two transport models, two prior emission fields, and three background estimates were conducted. Assume μ_i and σ_i represent the posterior emission estimate and its associated 1-sigma error for the i th inversion. Our final estimate of emissions and its associated uncertainty discussed in the text were calculated as the mean posterior emission and the 2-sigma uncertainty ($2\sigma_t$) derived from Eq. (1).

$$\sigma_t = \sqrt{\frac{{\sigma_1}^2+{\sigma_2}^2+\cdots+{\sigma_{12}}^2}{12} + {\sigma_s}^2} \quad (1)$$

where σ_s denotes 1 sigma spread or variability of the posterior emissions derived from all 12 inversions.

Results and discussion

Declining SF_6 emissions from the U.S.

The U.S. recognized that it had significant emissions of SF_6 in the 1990s and has taken steps to reduce its national emissions. In the U.S., 60 – 80% of SF_6 emissions have historically been from the ETD sector (Us Epa (United States Environmental Protection Agency), 2022b) (Fig. 1). Outside the ETD sector, smaller amounts of SF_6 are used in semiconductor manufacturing processes as a source of fluorine to etch patterns onto chips and to clean thin film deposition chambers, and SF_6 is also used as a cover gas in magnesium production and casting processes to prevent rapid oxidation of molten magnesium. Both of these uses result in emissions. SF_6 emissions from magnesium processes accounted for roughly 15 – 30 % of the U.S. total emissions reported by EPA between 1990 and 2018 (Fig. 1). While the magnitude of SF_6 emissions from the electronics manufacturing sector has not changed much over time, its share of total U.S. SF_6 emissions has increased from 2% in 1990 to 14% in 2018 as emissions from other industries have decreased.

Since 1999, the U.S. EPA has worked with the electric power industry through the voluntary SF_6 Emission Reduction Partnership for Electric Power Systems to identify, recommend, and implement cost-effective solutions to reduce SF_6 emissions. There have also been regulations at the state level to reduce SF_6 emissions from ETD (Us Epa (United States Environmental Protection Agency), 2022b). In addition, the EPA operated voluntary partnership programs with the semiconductor and magnesium industries from the late 1990s through 2010 to understand and reduce their emissions. These national- and state- level mitigation strategies, along with an increase in the market price of SF_6 during the 1990s, have resulted in a substantial reduction in total U.S. SF_6 emissions since 1990 (Us Epa (United States Environmental Protection Agency), 2022b) (Fig. 1). In addition, before 2011, SF_6 was likely emitted from an SF_6 production plant that ceased producing SF_6 in 2010, according to data reported to the U.S. EPA. Total U.S. SF_6 emissions estimated by the EDGARv6.0 showed an absolute decline over this period similar to that in the EPA GHGI, but EDGAR emissions were substantially larger on average (Fig. 1).

https://doi.org/10.5194/egusphere-2022-862
Preprint. Discussion started: 15 September 2022

Consistent with the inventory reports, the independent, atmospheric observation-based results presented here suggest a large decline of U.S. total SF_6 emissions, confirming the success of U.S. SF_6 emission mitigation efforts. The atmospheric observation-based emissions declined from 0.93 ($\pm 0.19, 2\sigma$) Gg yr^{-1} in 2007 – 2008 to 0.39 ($\pm 0.09, 2\sigma$) Gg yr^{-1} in 2017 – 2018 (Table 1 and Fig. 1). The 0.54 ± 0.15 (2σ) Gg yr^{-1} drop in SF_6 emissions from 2007 – 2008 to 2017 – 2018 is equivalent to reduction of 41 ± 11 million tons of CO_2 emission.

Although both the atmosphere-based top-down and inventory-based bottom-up estimates show declining trends for total U.S. SF_6 emissions, the estimated emission magnitudes are quite different. In 2007 – 2008, the atmosphere-based emissions fall between the EDGARv6.0 and EPA's GHGI estimates; but the difference between the atmosphere-based estimate and EDGARv6.0 increases over time, whereas the difference between the atmosphere-derived estimate and EPA's inventory decreases over time. After 2011, the atmosphere-based emission estimates are 0.93 ($\pm 0.07, 2\sigma$) Gg yr^{-1} (a factor of 3.4) lower than EDGARv6.0 and only about 0.15 ($\pm 0.07, 2\sigma$) Gg yr^{-1} (35%) higher than the EPA's GHGI (Us Epa (United States Environmental Protection Agency), 2022b). The improved agreement between the atmosphere-based estimates and EPA GHGI may be associated with more accurate emission information used to inform the EPA's GHGI after 2010. Before 2011, the SF_6 emission estimate in the EPA GHGI was primarily informed by reporting through the voluntary Partnership Programs between EPA and various industries (Rand, 2012) described above. In 2011, EPA established its greenhouse gas reporting program (GHGRP), requiring facility-based reporting of greenhouse gas (GHG) data and other relevant information from large GHG emission sources ($\geq$ 25,000 CO_2-equivalent metric tons of GHG emissions per year). Although smaller emitters are not required to report their emissions, this program provides more complete emission information than had been available prior to 2011. For example, from 1999 to 2010, ETD facilities representing an estimated 60% of the emitting activity reported their SF_6 emissions to EPA through EPA's voluntary reporting program. After 2010, ETD facilities representing an estimated 70% of the emitting activity began reporting their emissions to EPA under the GHGRP (16).

A variety of factors may be contributing to the difference observed between the SF_6 emissions estimates from atmospheric measurements and the estimates developed for the U.S. EPA GHGI. The largest potential contributor to the difference is a possible underestimate by the GHGI of emissions from ETD facilities that do not report to EPA, or that did not report to EPA until they were required to report by the GHGRP starting in 2011. Emissions from non-reporting facilities are currently estimated based on the uncertain assumption that the emission rate per mile of transmission line (transmission mile) for non-reporting facilities has been the same, on average, as that for reporting facilities in each year of the time series. However, the emission rate per transmission mile has varied significantly across facilities and over time due to a variety of factors, including the age of the electrical equipment, maintenance practices, local regulations, and the quantity of SF_6-containing equipment per transmission mile (SF_6 nameplate capacity) (16). Among reporting facilities, the emission rate has fallen from an average of 0.7 kg per transmission mile in 1999 to 0.2 kg per transmission mile in recent years (16), with emission rates declining most quickly in the first three years of reporting (i.e., 1999-2001 for Partners, 2011-2013 for facilities that began reporting under the GHGRP). This implies that reporting itself may drive emission reductions. Thus, it is plausible that the emission rate of non-reporting facilities has fallen more slowly than that of reporting facilities.

https://doi.org/10.5194/egusphere-2022-862
Preprint. Discussion started: 15 September 2022

In the years prior to 2011, there are several additional factors that may be contributing to the underestimate of SF_6 emissions by the GHGI, compared to the atmosphere-based estimates. One potentially significant factor is that the GHGI does not currently account for SF_6 emissions from the SF_6 production plant that operated in Metropolis, Illinois, through 2010. This plant never reported its emissions to EPA; but based on production capacity data for the plant from 2006 and the broad range of emission factors observed for production of SF_6 and other fluorinated gases, the plant's SF_6 emissions would likely have ranged between 0.03 and 0.3 Gg yr^{-1}. Notably, the region showing the largest drop in the atmosphere-derived emissions between 2008 and 2011-2018 includes Metropolis, Illinois (Fig. S2). Although emissions from this plant have not been included in previous GHGIs, the discrepancy highlighted here points to potential significant contributions from this plant (and other fluorinated gas production facilities) that will be included in future submissions of the GHGI.

Other factors that may account for a small portion of the post-2011 difference is an underestimate of emissions of SF_6 from electronics manufacturing by a factor of 2 (equivalent to ~ 0.02 Gg yr^{-1}). In the GHGI (16), the EPA adjusted the time series of GHGRP-reported data for 2011 through 2013 to ensure time-series consistency using a series of calculations that took into account the characteristics of a facility (e.g., wafer size and abatement use) and updated default emission factors and destruction and removal efficiencies. These updates reflected improved activity data and not changes to emission rates, and resulted in an increase in SF_6 emissions estimates by 95% from electronics manufacturing. Finally, a similar improvement for time series consistency is planned for pre-2011 estimates and is expected to result in a similar relative increase in estimated SF_6 emissions from the electronics sector for those years.

U.S. regional SF_6 emissions

We also investigated regional emissions derived from atmospheric inversions and from EPA's recently created Inventory of U.S. Greenhouse Gas Emission and Sinks by State (Us Epa (United States Environmental Protection Agency), 2022a) to understand the distribution of SF_6 emissions and how various regions contribute to the difference between the atmosphere- and inventory-derived U.S. total emissions. Note that the EPA GHGI was only able to allocate 20 – 30 % of ETD emissions to a single state by facility location (i.e. when the facility was only in one state). The remaining emission was distributed based on a national average emission factor (lbs of SF_6 per transmission mile). Because of this limited regional resolution, we expect some limitations in the regional estimates of the GHGI. However, this comparison with atmosphere-base estimates helps assess the robustness of the regional estimates.

The atmosphere-based emission estimates suggest that about 80% of the U.S. total SF_6 emissions were contributed by three regions: the northeast, central north, and central south (Table 1; Figs. 2 and S2). Regional SF_6 emissions corresponding to the GHGI calculated using the EPA's Inventory of U.S. Greenhouse Gas Emission and Sinks by State (Us Epa (United States Environmental Protection Agency), 2022a) were distributed slightly differently. For the southeast, west, and mountain regions, EPA's regional emissions agree well with emissions estimated from atmospheric observations, but they are lower than the atmosphere-derived emissions in the northeast for the entire study period and in the central north and central south during 2007 – 2010. Such regional differences were expected due to the limited regional resolution of the GHGI

https://doi.org/10.5194/egusphere-2022-862
Preprint. Discussion started: 15 September 2022

for emissions from ETD. For regions that predominantly had emissions from the ETD sector, the difference is likely more dependent on how similar the ETD emissions in the region are to the national average. This method could result in an underestimate of emissions in the regions like the northeast where the average emission rate is expected to be higher than the national average based on historical data submitted to the EPA by facilities in the region. Higher regional emission rates in the northeast could be due in part to the region containing more gas-insulated equipment per transmission mile and the presence of older transmission systems (i.e. older, leakier equipment). The national average emission factor may be more appropriate for the mountain, central north, and central south regions. This is because regional emission factors that are based only on GHGRP reported emissions from facilities that reside entirely within the region, are similar to a national average in these regions. Better agreement in the western region may be also associated with the incorporation of the California Air Resource Board estimate for SF_6 from California in the GHGI.

For the central north and central south regions, the atmosphere-derived emissions were higher in 2007 – 2010 and show a larger declining trend than the EPA GHGI. The larger discrepancy in the central north and central south before 2011 may be due in part to the unaccounted emissions by GHGI from the SF_6 production facility in Metropolis, Illinois, described above, which ceased producing SF_6 in 2010. This facility is located right at the border between the central north and central south regions, so it is likely that emissions from it could have been attributed to one or both adjacent regions in the atmospheric inversions.

Significant seasonality detected in U.S. SF_6 emissions

The monthly SF_6 emissions derived from our inverse analysis of atmospheric concentration measurements reveal a prominent seasonal cycle with higher emissions in winter for all 12 years of this analysis (Fig. 3). On average, the magnitude of winter SF_6 emissions is about a factor of 2 larger than summer emissions summed across the contiguous U.S. (Fig. 3). This seasonality is most likely from the use, servicing, and disposal of ETD equipment, as SF_6 emissions from magnesium production, electronics production, and manufacturing of ETD equipment are expected to be aseasonal. Consistent with this hypothesis, winter-to-summer ratios of total U.S. SF_6 emissions derived for individual years significantly correlate at a 99% confidence level ($r = 0.77$; $P = 0.003$) with the annual fractions of national emissions contributed by the ETD sector reported by EPA (Fig. 3). Moreover, this robust relationship also holds regionally ($r = 0.89$; $P = 0.02$) (Fig. 3). The largest seasonal variation in emissions is detected in the southeast and central south regions of the U.S., where the ETD sector accounted for more than 85% of the regional total emissions (Figs. 2 and 3). In these southern regions, the winter emissions were higher than summer emissions by more than a factor of 2, whereas in the central north, where the ETD sector accounted for about 50% of the regional total emissions, the mean winter-to-summer emission ratio was less than 1.5 (Figs. 2 and 3).

The enhanced winter emissions in the southern states are consistent with the fact that more servicing is performed on electrical equipment and transmission lines over this region in the cooler months (information provided by Mr. B. Lao at the DILO Company, Inc.), when electricity usage is low (Us Eia (Energy Information Administration), 2020). This suggests that the enhanced seasonal SF_6 emission may be associated with the season during which electrical equipment repair and servicing is enhanced. In the northern states, the higher winter than summer emissions may

https://doi.org/10.5194/egusphere-2022-862
Preprint. Discussion started: 15 September 2022

relate to increased leakage through more brittle seals in the aging electrical transmission equipment due to increased thermal contraction in winter (Du et al., 2020). This winter-to-summer ratios is somewhat higher in the northeast than in the other northern states, which may reflect the fact that the electrical power grid is denser (Us Federal Emergency Management Agency, 2008) and ETD is the primary emitting source of SF_6 over the region (Figs. 2 and 3).

Given that the ETD sector may be the primary cause for seasonally-varying emissions in the U.S., we next assessed changes in seasonality over time and their implication for changes in sector-based emissions from 2007 to 2018. The most notable feature of the time series (Fig. S3) is that the largest seasonal cycle occurred in 2009 when the economic recession took place. The 2009 recession resulted in a significant drop in the production of magnesium and electronics (Us Epa (United States Environmental Protection Agency), 2021), but little (if any) change to the ETD infrastructure and associated servicing practices is likely to have occurred. Thus, ETD emissions represent a larger fraction of the total U.S. SF_6 emissions in that year. In addition, the winter-to-summer emission ratios appear smaller before the 2009 peak (i.e., in 2007 – 2008) than after it (in 2011 – 2018). This may imply that emissions from the ETD sector accounted for a growing fraction of total emissions through this period.

Conclusions and implications

SF_6 is a potent industrially-produced greenhouse gas with an extremely long atmospheric lifetime. It is a trace gas that is primarily used in the electrification of the energy sector. In the past five decades, global emissions, concentrations, and radiative forcing of SF_6 have substantially increased due to growing energy demand. Without effective emission mitigation efforts worldwide, the climate impact of SF_6 will continue to rise in the future. In contrast to the global emission trend, U.S. SF_6 emissions have decreased substantially since the 1990s. These decreases are documented in EPA's emission inventories reported annually to the UNFCCC and in the new results reported here from an inverse analysis of atmosphere concentration measurements. These independently-derived U.S. emission records demonstrate substantial success by U.S. industry in coordination with the EPA in mitigating SF_6 emissions.

The magnitude of SF_6 emissions derived from atmospheric inversions are higher than those reported in the EPA GHGI but lower than EDGAR; but the difference between the EPA GHGI and atmosphere-derived estimates become substantially smaller after 2011 when national GHG reporting became mandatory, implying that that the shift from voluntary to mandatory emission reporting by industry increased the accuracy of the inventory. However, differences remain between the emissions estimated from these independent methods, which may relate to the uncertain assumptions about ETD-related emission rates per mile from non-reporting facilities in the GHGI. Although the U.S. GHGI may underestimate SF_6 emissions, its contribution to the global "missing" source of SF_6 is small. More specifically, the total SF_6 emissions summed from all reporting countries to the UNFCCC are only half of the global emissions derived from global-scale observed concentration trends; in other words, there are ~ 4 Gg SF_6 yr^{-1} or 100 million tons of CO_2-equivalent per year of SF_6 emissions still "missing" in the global GHG accounting system. The underestimate of the U.S. GHGI only contributed 14% in 2007 – 2008 and only 3% after 2011 to this global SF_6 emission gap, implying either large underreporting of SF_6 emissions from other countries or large emissions from non-reporting countries.

https://doi.org/10.5194/egusphere-2022-862
Preprint. Discussion started: 15 September 2022

Regional emissions from atmospheric inversions were compared with the recently available disaggregation of the U.S. GHGI by state to provide an initial assessment on the emission distribution of SF_6 estimated from the GHGI. Good agreement was noted in some regions but not others. Combining the spatial discrepancies with processes used for constructing the GHGI, we were able to identify regions where applying a national average emission factor is inappropriate and a facility (the SF_6 production plant in Metropolis, Illinois) whose historical emissions are currently not accounted for but may have been significant.

Finally, the atmosphere-derived results further suggest a strong seasonal cycle in SF_6 emissions from electric power transmission and distribution for the first time, with wintertime emissions twice as large as summertime emissions. This seasonal cycle is thought to be strongest in southern states, where servicing of ETD equipment is typically performed in winter. The seasonal cycle is likely enhanced additionally by increased leakage from ETD equipment during the winter, when cold weather makes sealing materials more brittle and therefore less effective. This newly discovered seasonal emission variation implies that further larger reductions of SF_6 emission in the U.S. might be achievable through efforts to minimize losses during equipment maintenance and repairs, and through the use of improved sealing materials in ETD equipment.

The 2019 Refinements to the 2006 IPCC Guidelines for National Greenhouse Gas Inventories suggest that atmospheric inversion-derived emissions be considered in the quality assurance, quality control and verification of the national GHG inventory reporting. It is anticipated that the consideration of an independent estimate will lead to more accurate inventories. The work presented here, however, suggests that a collaboration between these communities can provide much more. In the case of SF_6, the result has been not only an improved understanding of emission magnitudes, but also a better grasp of the processes that lead to emissions and the identification of substantial new emission mitigation opportunities, thereby pointing the way towards a more effective and efficient means to minimize and reduce national greenhouse gas emissions.

Data availability

Atmospheric SF_6 observations used in this analysis are publicly available at https://gml.noaa.gov/ccgg/obspack/data.php. The marine boundary layer reference for SF_6 can be downloaded from https://gml.noaa.gov/ccgg/mbl/data.php. Atmospheric observation-derived US national and regional emissions from this analysis are accessible through the US Emission Tracker for Potent GHGs (https://gml.noaa.gov/hats/US_emissiontracker/?gas=HFC134a). SF_6 emissions reported to the GHGR are available at https://www.epa.gov/enviro/greenhouse-gas-customized-search.

Author contributions

LH performed the analysis and wrote the paper with DO, SB, and SM. Significant edits and inputs are also from PD and ED. DO and SB made and provided EPA SF_6 emission estimates. PD, SM, and LH initiated this project. ED led the NOAA SF_6 measurements. PD coordinated the discussion between NOAA and EPA colleagues. AA led the NOAA tower sampling network, provided the

https://doi.org/10.5194/egusphere-2022-862
Preprint. Discussion started: 15 September 2022

4D empirical background estimates of SF_6 and WRF-STILT footprints. KT and GD helped with improving the inversion code. KT and LH computed the HYSPLIT footprints. CS led the NOAA aircraft sampling network. LA contributed the construction of EPA SF_6 emission estimates. AC contributed to NOAA SF_6 measurements.

The views expressed in this article are those of the authors and do not necessarily represent the views or policies of the U.S. Environmental Protection Agency.

Acknowledgement

This work was funded in part by the Grantham Foundation, NOAA Climate Program Office's Atmospheric Chemistry, Carbon Cycle, and Climate (AC4) and Climate Observations and Monitoring (COM) programs (NA21OAR4310233), and the NOAA Cooperative Agreement with CIRES, NA17OAR4320101. We thank Mr. Billy Lao at the DILO company, Inc. for insights on the timing of repairing and servicing of electrical equipment. We thank Dr. Bradley Hall for maintaining the primary SF_6 calibration scale for all NOAA SF_6 measurements. We thank Jon Kofler, Kathryn McKain, Don Neff, Sonja Wolter, Jack Higgs, Molly Crotwell, Patrick Lang, Eric Moglia, and Monica Madronich for facilitating flask sampling and measurements. We thank Dr. Andy Jacobson for providing SF_6 simulations from the SF_6 Model Inter-comparison Project.

References

Crippa, M., Guizzardi, D., Muntean, M., Schaaf, E., Lo Vullo, E., Solazzo, E., Monforti-Ferrario, F., Olivier, J., and Vignati, E.: EDGAR v6.0 Greenhouse Gas Emissions [dataset], 2021.

Denning, A. S., Holzer, M., Gurney, K. R., Heimann, M., Law, R. M., Rayner, P. J., Fung, I. Y., Fan, S.-M., Taguchi, S., Friedlingstein, P., Balkanski, Y., Taylor, J., Maiss, M., and Levin, I.: Three-dimensional transport and concentration of SF6 A model intercomparison study (TransCom 2), Tellus B: Chemical and Physical Meteorology, 51, 266-297, 10.3402/tellusb.v51i2.16286, 1999.

Du, B., Zhang, Z., Qiao, Y., Suo, S., Luo, H., and Li, X.: Online sealing of SF6 leak for Gas insulated switchgear, IOP Conference Series: Earth and Environmental Science, 514, 042021, 10.1088/1755-1315/514/4/042021, 2020.

Forster, P., Storelvmo, T., Armour, K., Collins, W., Dufresne, J. L., Frame, D., Lunt, D. J., Mauritsen, T., Palmer, M. D., Watanabe, M., Wild, M., and Zhang, H.: The Earth's Energy Budget, Climate Feedbacks, and Climate Sensitivity, in: Climate Change 2021: The Physical Science Basis. Contribution of Working Group I to the Sixth Assessment Report of the Intergovernmental Panel on Climate Change, edited by: Masson-Delmotte, V., Zhai, P., Pirani, A., Connors, S. L., Pean, C., Berger, S., Caud, N., Chen, Y., Goldfarb, L., Gomis, M. I., Huang, M., Leitzell, K., Lonnoy, E., Matthews, J. B. R., Maycock, T. K., Waterfield, T., Yelekci, O., Yu, R., and Zhou, B., Cambridge University Press, 2021.

Fraser, P., Dunse, B., Krummel, P. B., Steele, P., and Derek, P.: Australian HFC, PFC, Sulfur Hexafluoride and Sulfuryl
Fluoride emissions, Report prepared for Australian Goverment Department of the Environment, by the centre for Australian Weather and Climate Research, CSIRO Oceans and Atmosphere Flagship, Aspendale, Austalia, 27, 2014.

https://doi.org/10.5194/egusphere-2022-862
Preprint. Discussion started: 15 September 2022

Gloor, M., Dlugokencky, E., Brenninkmeijer, C., Horowitz, L., Hurst, D. F., Dutton, G., Crevoisier, C., Machida, T., and Tans, P.: Three-dimensional SF6 data and tropospheric transport simulations: Signals, modeling accuracy, and implications for inverse modeling, Journal of Geophysical Research: Atmospheres, 112, https://doi.org/10.1029/2006JD007973, 2007.

Gulev, S. K., Thorne, P. W., Ahn, J., Dentener, F. J., Domingues, C. M., Gerland, S., Gong, D., Kaufman, D. S., Nnamchi, H. C., Quaas, J., Rivera, J. A., Sathyendranath, S., Smith, S. L., Trewin, B., vo Shuckmann, K., and Vose, R. S.: Changing State of the Climate System, in: Climate Change 2021: The Physical Science Basis. Contribution of Working Group I to the Sixth Assessment Report of the Intergovernmental Panel on Climate Change, edited by: Masson-Delmotte, V., Zhai, P., Pirani, A., Connors, S. L., Pean, C., Berger, S., Caud, N., Chen, Y., Goldfarb, L., Gomis, M. I., Huang, M., Leitzell, K., Lonnoy, E., Matthews, J. B. R., Maycock, T. K., Waterfield, T., Yelekci, O., Yu, P., and Zhou, B., Cambridge University Press, 2021.

Henne, S., Brunner, D., Oney, B., Leuenberger, M., Eugster, W., Bamberger, I., Meinhardt, F., Steinbacher, M., and Emmenegger, L.: Validation of the Swiss methane emission inventory by atmospheric observations and inverse modelling, Atmos. Chem. Phys., 16, 3683-3710, 10.5194/acp-16-3683-2016, 2016.

Hu, L., Montzka, S. A., Kaushik, A., Andrews, A. E., Sweeney, C., Miller, J., Baker, I. T., Denning, S., Campbell, E., Shiga, Y. P., Tans, P., Siso, M. C., Crotwell, M., McKain, K., Thoning, K., Hall, B., Vimont, I., Elkins, J. W., Whelan, M. E., and Suntharalingam, P.: COS-derived GPP relationships with temperature and light help explain high-latitude atmospheric CO₂ seasonal cycle amplification, Proceedings of the National Academy of Sciences, 118, e2103423118, 10.1073/pnas.2103423118, 2021.

Hu, L., Montzka, S. A., Lehman, S. J., Godwin, D. S., Miller, B. R., Andrews, A. E., Thoning, K., Miller, J. B., Sweeney, C., Siso, C., Elkins, J. W., Hall, B. D., Mondeel, D. J., Nance, D., Nehrkorn, T., Mountain, M., Fischer, M. L., Biraud, S. C., Chen, H., and Tans, P. P.: Considerable contribution of the Montreal Protocol to declining greenhouse gas emissions from the United States, Geophysical Research Letters, 44, 2017GL074388, 10.1002/2017GL074388, 2017.

Hu, L., Andrews, A. E., Thoning, K. W., Sweeney, C., Miller, J. B., Michalak, A. M., Dlugokencky, E., Tans, P. P., Shiga, Y. P., Mountain, M., Nehrkorn, T., Montzka, S. A., McKain, K., Kofler, J., Trudeau, M., Michel, S. E., Biraud, S. C., Fischer, M. L., Worthy, D. E. J., Vaughn, B. H., White, J. W. C., Yadav, V., Basu, S., and van der Velde, I. R.: Enhanced North American carbon uptake associated with El Niño, Science Advances, 5, eaaw0076, 10.1126/sciadv.aaw0076, 2019.

Hu, L., Montzka, S. A., Miller, B. R., Andrews, A. E., Miller, J. B., Lehman, S. J., Sweeney, C., Miller, S. M., Thoning, K., Siso, C., Atlas, E. L., Blake, D. R., de Gouw, J., Gilman, J. B., Dutton, G., Elkins, J. W., Hall, B., Chen, H., Fischer, M. L., Mountain, M. E., Nehrkorn, T., Biraud, S. C., Moore, F. L., and Tans, P.: Continued emissions of carbon tetrachloride from the United States nearly two decades after its phaseout for dispersive uses, Proceedings of the National Academy of Sciences, 113, 2880-2885, 10.1073/pnas.1522284113, 2016.

Hu, L., Montzka, S. A., Miller, J. B., Andrews, A. E., Lehman, S. J., Miller, B. R., Thoning, K., Sweeney, C., Chen, H., Godwin, D. S., Masarie, K., Bruhwiler, L., Fischer, M. L., Biraud, S. C., Torn, M. S., Mountain, M., Nehrkorn, T., Eluszkiewicz, J., Miller, S., Draxler, R. R., Stein, A. F., Hall, B. D., Elkins, J. W., and Tans, P. P.: U.S. emissions of HFC-134a derived for 2008–2012 from an extensive flask-air sampling network, Journal of Geophysical Research: Atmospheres, 2014JD022617, 10.1002/2014JD022617, 2015.

https://doi.org/10.5194/egusphere-2022-862
Preprint. Discussion started: 15 September 2022

549 Janssens-Maenhout, G.: EDGARv4.2 Emission Maps [dataset], 2011.
550 Levin, I., Naegler, T., Heinz, R., Osusko, D., Cuevas, E., Engel, A., Ilmberger, J., Langenfelds,
551 R. L., Neininger, B., Rohden, C. v., Steele, L. P., Weller, R., Worthy, D. E., and Zimov, S. A.:
552 The global SF₆ source inferred from long-term high precision atmospheric
553 measurements and its comparison with emission inventories, Atmos. Chem. Phys., 10, 2655-
554 2662, 10.5194/acp-10-2655-2010, 2010.
555 Maksyutov, S., Eggleston, S., HHun Woo, J., Fang, S., Witi, J., Gillenwater, M., Goodwin, J.,
556 and Tubiello, F.: Chapter 6: Quality Assurance / Quanlity Control and Verification,
557 Intergovernmental Panel on Climate Change (IPCC), Kyoto, Japan, 2019.
558 Manning, A. J., Stanley, K., Redington, A., O'Doherty, S., and Young, D.: Methodology Report
559 Verification of Emissions using Atmospheric Observations, 2017.
560 Michalak, A. M., Hirsch, A., Bruhwiler, L., Gurney, K. R., Peters, W., and Tans, P. P.:
561 Maximum likelihood estimation of covariance parameters for Bayesian atmospheric trace gas
562 surface flux inversions, Journal of Geophysical Research: Atmospheres, 110, D24107,
563 10.1029/2005jd005970, 2005.
564 Nehrkorn, T., Eluszkiewicz, J., Wofsy, S., Lin, J., Gerbig, C., Longo, M., and Freitas, S.:
565 Coupled weather research and forecasting–stochastic time-inverted lagrangian transport (WRF–
566 STILT) model, Meteorology and Atmospheric Physics, 107, 51-64, 10.1007/s00703-010-0068-x,
567 2010.
568 Nevison, C., Andrews, A., Thoning, K., Dlugokencky, E., Sweeney, C., Miller, S., Saikawa, E.,
569 Benmergui, J., Fischer, M., Mountain, M., and Nehrkorn, T.: Nitrous Oxide Emissions Estimated
570 With the CarbonTracker-Lagrange North American Regional Inversion Framework, Global
571 Biogeochemical Cycles, 32, 463-485, doi:10.1002/2017GB005759, 2018.
572 Orbe, C., Waugh, D. W., Montzka, S., Dlugokencky, E. J., Strahan, S., Steenrod, S. D., Strode,
573 S., Elkins, J. W., Hall, B., Sweeney, C., Hintsa, E. J., Moore, F. L., and Penafiel, E.:
574 Tropospheric Age-of-Air: Influence of SF6 Emissions on Recent Surface Trends and Model
575 Biases, Journal of Geophysical Research: Atmospheres, 126, e2021JD035451,
576 https://doi.org/10.1029/2021JD035451, 2021.
577 Ottinger, D., Averyt, M., and Harris, D.: US consumption and supplies of sulphur hexafluoride
578 reported under the greenhouse gas reporting program, Journal of Integrative Environmental
579 Sciences, 12, 5-16, 10.1080/1943815X.2015.1092452, 2015.
580 Peters, W., Krol, M. C., Dlugokencky, E. J., Dentener, F. J., Bergamaschi, P., Dutton, G.,
581 Velthoven, P. v., Miller, J. B., Bruhwiler, L., and Tans, P. P.: Toward regional-scale modeling
582 using the two-way nested global model TM5: Characterization of transport using SF6, Journal of
583 Geophysical Research: Atmospheres, 109, D19314, 10.1029/2004jd005020, 2004.
584 Rand, S.: EPA's SF6 Emission Reduction Partnership for Electric Power Systems, 2012.
585 Ray, E. A., Moore, F. L., Elkins, J. W., Rosenlof, K. H., Laube, J. C., Röckmann, T., Marsh, D.
586 R., and Andrews, A. E.: Quantification of the SF6 lifetime based on mesospheric loss measured
587 in the stratospheric polar vortex, Journal of Geophysical Research: Atmospheres, 122, 4626-
588 4638, https://doi.org/10.1002/2016JD026198, 2017.
589 Rigby, M., Mühle, J., Miller, B. R., Prinn, R. G., Krummel, P. B., Steele, L. P., Fraser, P. J.,
590 Salameh, P. K., Harth, C. M., Weiss, R. F., Greally, B. R., O'Doherty, S., Simmonds, P. G.,
591 Vollmer, M. K., Reimann, S., Kim, J., Kim, K. R., Wang, H. J., Olivier, J. G. J., Dlugokencky,
592 E. J., Dutton, G. S., Hall, B. D., and Elkins, J. W.: History of atmospheric SF₆ from
593 1973 to 2008, Atmos. Chem. Phys., 10, 10305-10320, 10.5194/acp-10-10305-2010, 2010.

https://doi.org/10.5194/egusphere-2022-862
Preprint. Discussion started: 15 September 2022

Rodgers, C. D.: Inverse Methods for Atmospheric Sounding, Inverse Methods for Atmospheric Sounding, 10.1142/3171,

Schuh, A. E., Jacobson, A. R., Basu, S., Weir, B., Baker, D., Bowman, K., Chevallier, F., Crowell, S., Davis, K. J., Deng, F., Denning, S., Feng, L., Jones, D., Liu, J., and Palmer, P. I.: Quantifying the Impact of Atmospheric Transport Uncertainty on CO2 Surface Flux Estimates, Global Biogeochemical Cycles, 33, 484-500, https://doi.org/10.1029/2018GB006086, 2019.

Simmonds, P. G., Rigby, M., Manning, A. J., Park, S., Stanley, K. M., McCulloch, A., Henne, S., Graziosi, F., Maione, M., Arduini, J., Reimann, S., Vollmer, M. K., Mühle, J., O'Doherty, S., Young, D., Krummel, P. B., Fraser, P. J., Weiss, R. F., Salameh, P. K., Harth, C. M., Park, M. K., Park, H., Arnold, T., Rennick, C., Steele, L. P., Mitrevski, B., Wang, R. H. J., and Prinn, R. G.: The increasing atmospheric burden of the greenhouse gas sulfur hexafluoride (SF6), Atmos. Chem. Phys., 20, 7271-7290, 10.5194/acp-20-7271-2020, 2020.

Stein, A. F., Draxler, R. R., Rolph, G. D., Stunder, B. J. B., Cohen, M. D., and Ngan, F.: NOAA's HYSPLIT atmospheric transport and dispersion modeling system, Bulletin of the American Meteorological Society, 10.1175/BAMS-D-14-00110.1, 2015.

Hourly electricity consumption varies throughout the day and across seasons: https://www.eia.gov/todayinenergy/detail.php?id=42915#:~:text=During%20the%20winter%20months%2C%20hourly,for%20space%20heating%20or%20cooling, last access: Jul 7.

US EPA (United States Environmental Protection Agency): Inventory of U.S. Greenhouse Gas Emissions and Sinks: 1990-2019EPA 430-R-21-005, 2021.

Inventory of U.S. Greenhouse Gas Emissions and Sinks by State: https://www.epa.gov/ghgemissions/state-ghg-emissions-and-removals, last access: Jul 7.

US EPA (United States Environmental Protection Agency): Inventory of U.S. Greenhouse Gas Emissions and Sinks: 1990-2020EPA 430-R-22-003, 2022b.

United States transmission grid: https://en.wikipedia.org/wiki/North_American_power_transmission_grid#/media/File:UnitedStatesPowerGrid.jpg, last access: Apr 5.

Waugh, D. W., Crotwell, A. M., Dlugokencky, E. J., Dutton, G. S., Elkins, J. W., Hall, B. D., Hintsa, E. J., Hurst, D. F., Montzka, S. A., Mondeel, D. J., Moore, F. L., Nance, J. D., Ray, E. A., Steenrod, S. D., Strahan, S. E., and Sweeney, C.: Tropospheric SF6: Age of air from the Northern Hemisphere midlatitude surface, Journal of Geophysical Research: Atmospheres, 118, 11,429-411,441, https://doi.org/10.1002/jgrd.50848, 2013.

Weiss, R. F. and Prinn, R. G.: Quantifying greenhouse-gas emissions from atmospheric measurements: a critical reality check for climate legislation, Philosophical Transactions of the Royal Society A: Mathematical, Physical and Engineering Sciences, 369, 1925-1942, doi:10.1098/rsta.2011.0006, 2011.

https://doi.org/10.5194/egusphere-2022-862
Preprint. Discussion started: 15 September 2022

Table 1. US national and regional annual emissions of SF_6 (in Gg yr^{-1}) reported by EPA and derived from NOAA atmospheric measurements from this study. Errors derived from NOAA atmospheric measurements are expressed at a 95% confidence interval.

Year	National totals		Regions											
			Northeast		Southeast		Central North		Central South		Mountain		West	
	EPA	NOAA	EPA	NOAA	EPA	NOAA	EPA	NOAA	EPA	NOAA	EPA	NOAA	EPA	NOAA
2007	0.40	0.83±0.19	0.04	0.18±0.10	0.03	0.05±0.07	0.16	0.30±0.07	0.06	0.22±0.07	0.07	0.04±0.03	0.04	0.03±0.07
2008	0.37	1.03±0.26	0.05	0.22±0.10	0.02	0.09±0.07	0.13	0.34±0.14	0.06	0.28±0.09	0.06	0.06±0.04	0.03	0.04±0.06
2009	0.32	0.75±0.26	0.04	0.16±0.10	0.03	0.08±0.05	0.10	0.25±0.13	0.06	0.22±0.10	0.06	0.02±0.03	0.03	0.02±0.04
2010	0.32	0.63±0.16	0.04	0.12±0.04	0.02	0.05±0.03	0.11	0.20±0.08	0.06	0.12±0.04	0.06	0.05±0.02	0.03	0.08±0.04
2011	0.36	0.58±0.12	0.04	0.13±0.04	0.03	0.06±0.02	0.14	0.19±0.05	0.06	0.11±0.03	0.06	0.03±0.02	0.03	0.06±0.02
2012	0.30	0.40±0.11	0.04	0.09±0.05	0.03	0.04±0.03	0.10	0.13±0.03	0.05	0.08±0.03	0.05	0.03±0.02	0.03	0.04±0.02
2013	0.28	0.40±0.12	0.04	0.11±0.07	0.03	0.03±0.03	0.08	0.13±0.04	0.04	0.08±0.03	0.05	0.02±0.02	0.03	0.03±0.02
2014	0.29	0.48±0.14	0.04	0.15±0.09	0.03	0.05±0.03	0.09	0.13±0.04	0.05	0.08±0.03	0.05	0.03±0.02	0.03	0.03±0.02
2015	0.24	0.43±0.14	0.04	0.13±0.05	0.02	0.05±0.03	0.08	0.13±0.04	0.04	0.07±0.02	0.04	0.03±0.02	0.02	0.03±0.02
2016	0.26	0.38±0.11	0.04	0.12±0.04	0.03	0.04±0.02	0.10	0.11±0.04	0.04	0.07±0.02	0.04	0.02±0.01	0.02	0.02±0.01
2017	0.26	0.38±0.11	0.03	0.10±0.04	0.03	0.03±0.02	0.09	0.12±0.04	0.04	0.07±0.03	0.04	0.03±0.02	0.02	0.03±0.02
2018	0.25	0.40±0.11	0.03	0.10±0.02	0.03	0.06±0.03	0.09	0.13±0.04	0.04	0.07±0.03	0.04	0.02±0.01	0.02	0.02±0.02

https://doi.org/10.5194/egusphere-2022-862
Preprint. Discussion started: 15 September 2022

Figures

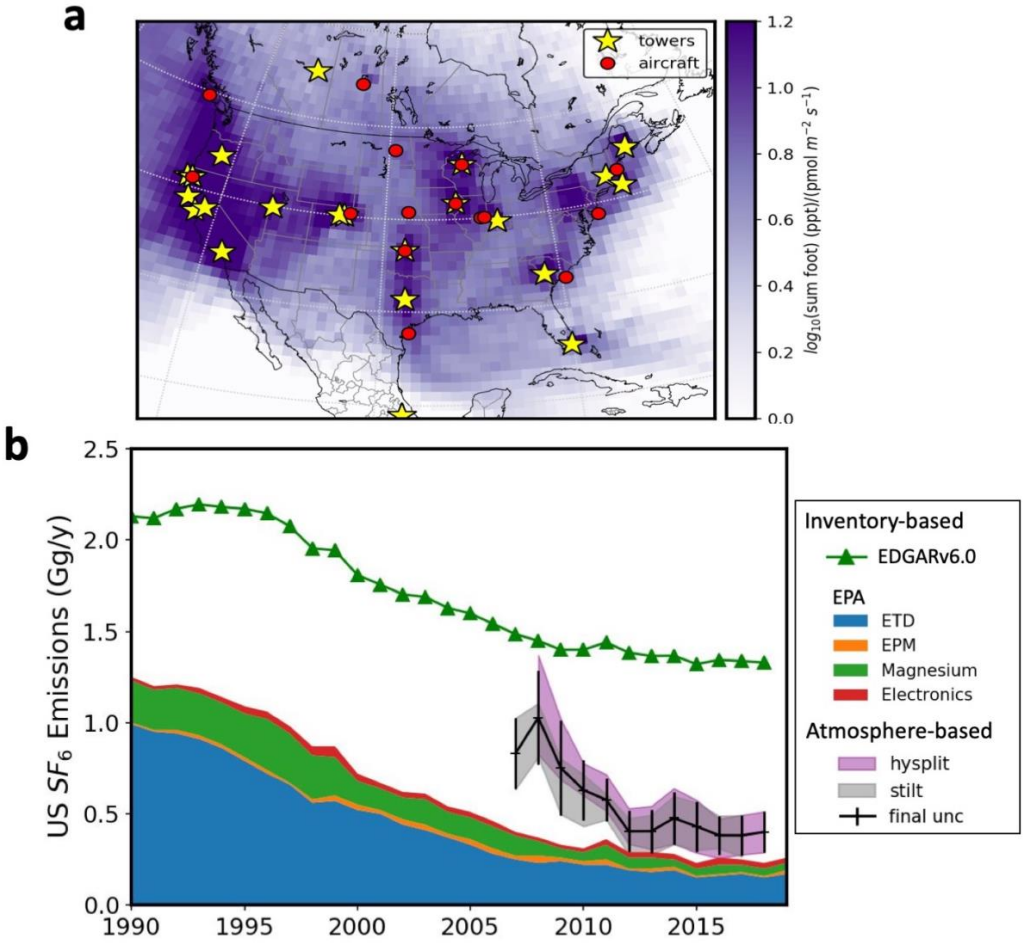

Fig. 1. US SF_6 emissions derived from atmospheric observations and reported by inventories. (a) Locations of atmospheric SF_6 measurements considered in the regional inversions; tower-based sampling is indicated as stars and airborne-profile sampling is denoted as circles. Sensitivity of the atmospheric SF_6 measurements to surface emissions is indicated on a log10 scale as purple shading. (b) US SF_6 emissions reported by EDGARv6.0 and EPA inventories and derived from atmospheric observations. National totals are shown from EDGARv6.0, whereas the EPA inventory is parsed out by sector, including electric power transmission and distribution (ETD), electrical equipment manufacturing (EPM), magnesium production, and electronics. Atmosphere-based emission estimates for the contiguous U.S. are derived with two different model analyses of the atmospheric observations using two difference transport simulations (HYSPLIT-NAMS in purple shading and WRF-STILT in gray shading). The black line with error bars indicates inversion ensemble annual means and an uncertainty at a 95% confidence interval.

https://doi.org/10.5194/egusphere-2022-862
Preprint. Discussion started: 15 September 2022

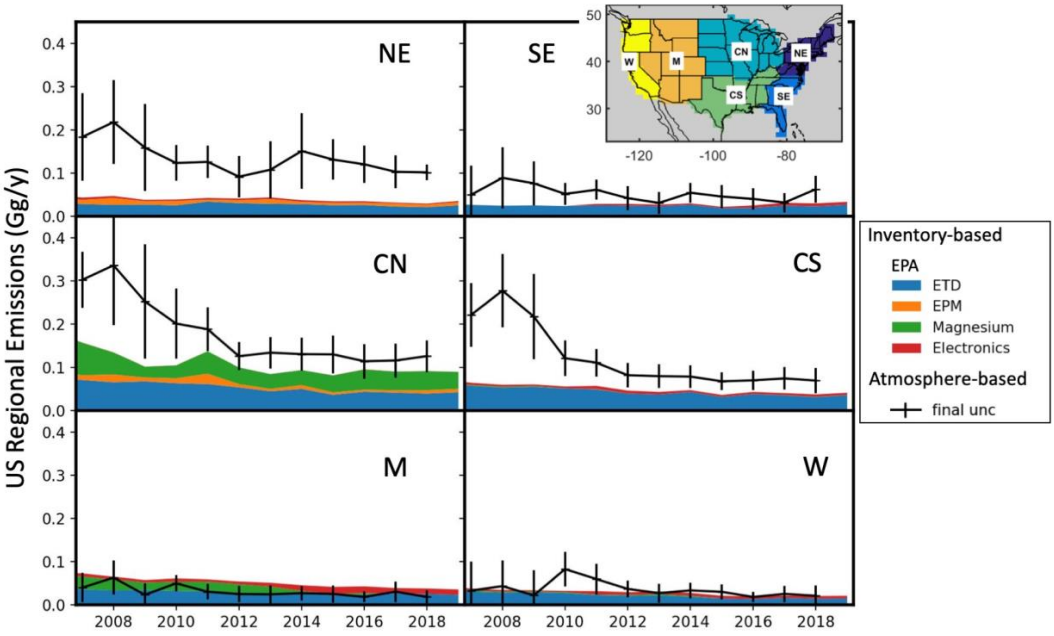

Fig. 2. Regional SF_6 emissions over the US, derived from atmospheric observations and reported by EPA by sectors, i.e., electrical transformation and distribution (ETD), electrical power manufacturing (EPM), magnesium production, and electronics. Atmosphere-based emission estimates (black lines) include uncertainties at a 95% confidence interval (vertical black bars).

https://doi.org/10.5194/egusphere-2022-862
Preprint. Discussion started: 15 September 2022

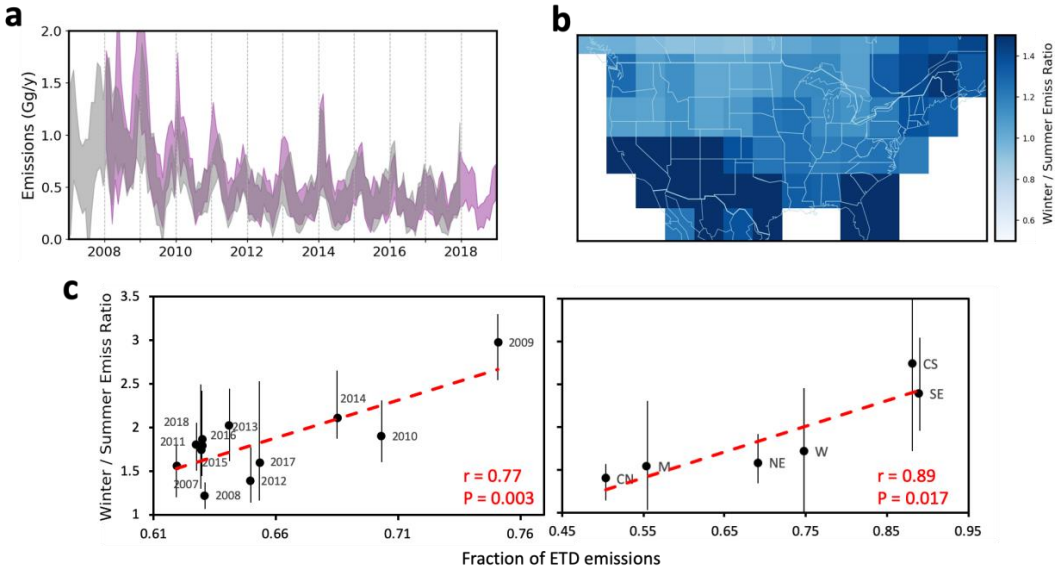

Fig. 3. Seasonal cycle of US SF_6 emissions derived from atmospheric observations. (a) Monthly emissions derived from atmospheric inversions using HYSPLIT-NAMS (in purple shading) and WRF-STILT (in gray shading) transport simulations. (b) The winter-to-summer emission ratios derived on a $5^o \times 5^o$ grid from atmospheric observations, averaged across all years and 12 inversion ensemble members. The winter and summer here are defined as Nov – Feb and May – Aug. (c) Atmosphere-derived winter-to-summer emission ratios versus the fraction of total U.S. SF_6 emissions from electric power transformation and distribution (ETD) reported by EPA. Left: the ETD emission fraction versus winter-to-summer emission ratios for annual national emissions; errorbars indicate the 2.5^{th} – 97.5^{th} percentile range from the 12 inversion ensembles. Right: the mean ETD emission fraction by region averaged between 2007-2018 versus winter-to-summer emission ratios for multi-year average regional emissions over the same period; errorbars indicate the 2.5^{th} – 97.5^{th} percentile range from the 12 inversion ensembles.